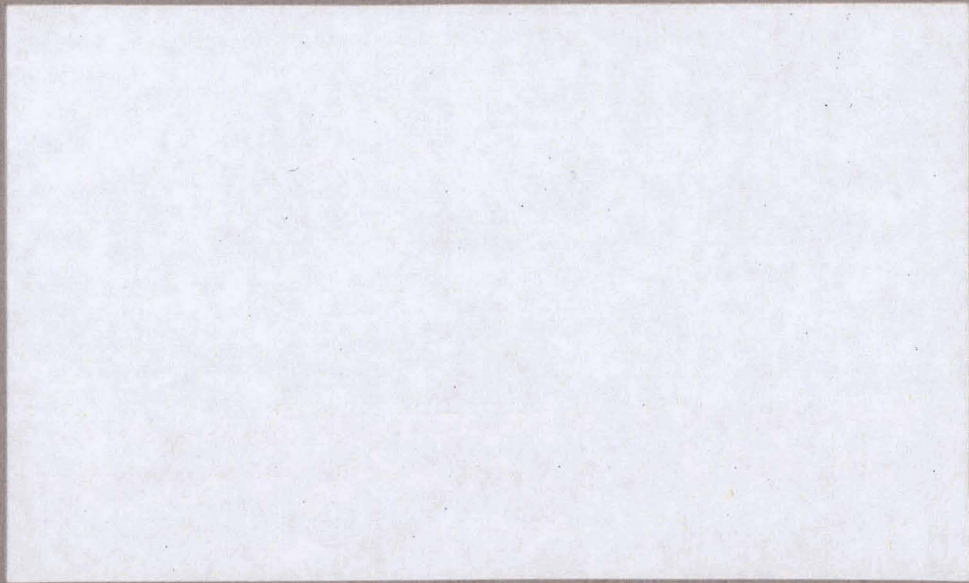


SEP 23 1963

FURITK - 678 ✓



ALLIS-CHALMERS



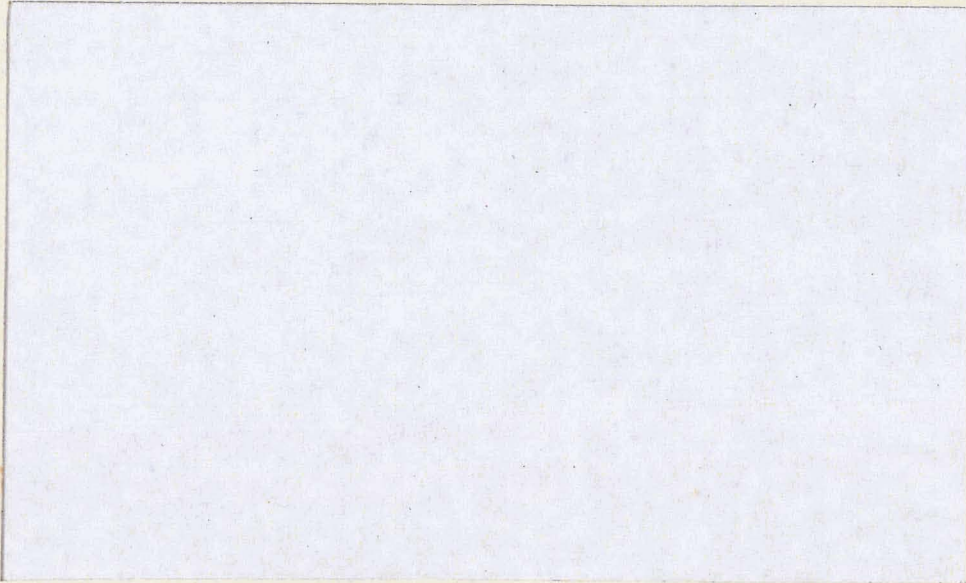
ATOMIC ENERGY DIVISION

DISCLAIMER

This report was prepared as an account of work sponsored by an agency of the United States Government. Neither the United States Government nor any agency Thereof, nor any of their employees, makes any warranty, express or implied, or assumes any legal liability or responsibility for the accuracy, completeness, or usefulness of any information, apparatus, product, or process disclosed, or represents that its use would not infringe privately owned rights. Reference herein to any specific commercial product, process, or service by trade name, trademark, manufacturer, or otherwise does not necessarily constitute or imply its endorsement, recommendation, or favoring by the United States Government or any agency thereof. The views and opinions of authors expressed herein do not necessarily state or reflect those of the United States Government or any agency thereof.

DISCLAIMER

Portions of this document may be illegible in electronic image products. Images are produced from the best available original document.



LEGAL NOTICE

This document was prepared under the sponsorship of the U.S. Atomic Energy Commission pursuant to the Joint Research and Development Program established by the Agreement for Cooperation signed November 8, 1958, between the Government of the United States of America and the European Atomic Energy Community (EURATOM). Neither the United States, the U.S. Atomic Energy Commission, the European Atomic Energy Community, the Euratom Commission, nor any person acting on behalf of either Commission:

- A. Makes any warranty or representation, express or implied, with respect to the accuracy, completeness or usefulness of the information contained in this document, or that the use of any information, apparatus, method, or process disclosed in this document may not infringe privately owned rights; or
- B. Assumes any liabilities with respect to the use of, or for damages resulting from the use of any information, apparatus, method or process disclosed in this document.

As used in the above, "person acting on behalf of either Commission" includes any employee or contractor of either Commission or employee of such contractor to the extent that such employee or contractor or employee of such contractor prepares, handles, disseminates, or provides access to, any information pursuant to his employment or contract with either Commission or his employment with such contractor.

JOINT US/EURATOM R&D PROGRAM

AT (11-1) ~~486~~ 1229

Shaped Burnable Poison Development Program
Under the Euratom Program

MASTER

QUARTERLY PROGRESS REPORT

DECEMBER 1, 1962 - FEBRUARY 28, 1963

Prepared for the

U. S. ATOMIC ENERGY COMMISSION
Under the US/EURATOM Agreement

ALLIS-CHALMERS
ATOMIC ENERGY DIVISION
MILWAUKEE 1, WISCONSIN
U. S. A.

April 10, 1963

Available from the
Office of Technical Services
Department of Commerce
Washington 25, D. C.

Facsimile Price \$ 2.60
Microfilm Price \$ 1.25

TABLE OF CONTENTS

	<u>Page</u>
List of Illustrations	iii
Project Statement	iv
1.0 Abstract	1
2.0 Principal Investigators	2
3.0 Statement of Problem	3
3.1 Nuclear Cross Section Data	3
3.2 Poison Demand Curves	3
3.3 Cylindrical Shaped Lumps	3
3.4 Fabrication of Al_2O_3 , Gd_2O_3 , and $Al_2O_3-Gd_2O_3$ Rods	3
3.5 $Al_2O_3-Gd_2O_3$ Reaction Studies	3
3.6 Fabrication of Gd_2O_3 Wafers	4
4.0 Description of Work, Computational and Fabrication Results	5
4.1 Nuclear Cross Section Data	5
4.2 Poison Demand Curves	8
4.3 Analytical Model for Depletion of Poison Cylinders	14
4.4 Reaction Study	17
4.5 Fabrication Development	19
4.6 Fabrication of Gd_2O_3 Wafers	22
5.0 Plans for Future Work	25
5.1 Poison Demand Curves and Control Requirements	25
5.2 Depletion of Poison Lump	25

	<u>Page</u>
5.3 Poison Lumps for Danger Coefficients	25
5.4 Reaction Studies	25
5.5 Fabrication Techniques	26
5.6 Danger Coefficient Samples	26
6.0 Conclusions	28
References	29

LIST OF ILLUSTRATIONS

<u>Fig. No.</u>	<u>Title</u>	<u>Page</u>
1.	Absorption Cross Section for Gd-155 and Gd-157 vs. Energy	7
2.	Absorption Cross Section for Gd vs. Energy	9
3.	Maxwellian Averaged Absorption Cross Section for Gd vs. Temperature	10
4.	Poison Demand Curves for Boiling Water Reactor with $H_2O/UO_2 = 2.6$	13
5.	Schedule of Progress Bar Graph	27

PROJECT STATEMENT

The United States and the European Atomic Energy Community (EURATOM), on May 29 and June 18, 1958, signed an agreement which provides a basis for cooperation in programs for the advancement of the peaceful applications of atomic energy. This agreement, in part, provides for the establishment of a Joint U.S. - Euratom research and development program which is aimed at reactors to be constructed in Europe under the Joint Program.

The work described in this report represents the Joint U.S. - Euratom effort which is in keeping with the spirit of cooperation in contributing to the common good by the sharing of scientific and technical information and minimizing the duplication of effort by the limited pool of technical talent available in Western Europe and the United States.

1.0 ABSTRACT

Nuclear cross section data for gadolinium, Gd-155, and Gd-157, were compiled. Average absorption cross sections were computed assuming Maxwellian thermal spectra for moderator temperatures from 70 F to 600 F.

Poison demand curves were computed for a boiling water reactor with an H₂O-to-UO₂ ratio of 2.6, U-235 enrichments from 1.8 w/o to 3.8 w/o, zirconium or stainless steel as clad, and fuel depletions in the range of 10,000 to 25,000 MWD/T.

Based on the above poison demand curves, poison lumps in the shape of cylinders are being investigated analytically. A calculational method is being developed for detailed depletion studies of cylinders.

Gadolinia, alumina, and Al₂O₃-Gd₂O₃ rods were formed and sintered at temperatures to 2700 F, in an air atmosphere for two to six hours. Investigations of reaction between Gd₂O₃ and Al₂O₃ were begun.

2.0 PRINCIPAL INVESTIGATORS

The following investigators were active on the program this quarter:

Pierre Descleve

Benjamin Fitts

Patrick Lacy

3.0 STATEMENT OF THE PROBLEM

Program activities this quarter have been divided into the following categories:

3.1 Nuclear Cross Section Data

Nuclear cross section data for gadolinium by isotope were reviewed. Absorption cross sections for Gd, Gd-155 and Gd-157 were computed as a function of energy and averaged over Maxwellian spectra as a function of temperature.

3.2 Poison Demand Curves

To provide a basis for selecting a poison lump shape, poison demand curves for eight fuel lattices were computed as a function of MWD/T for a large boiling water reactor.

3.3 Cylindrical Shaped Lumps

Based on the results of the poison demand calculations, detailed studies were initiated on neutron capture probabilities in cylindrical shaped poison lumps.

3.4 Fabrication of Al_2O_3 , and $Al_2O_3-Gd_2O_3$ Rods

To begin investigation of fabrication techniques, Al_2O_3 , Gd_2O_3 , and $Al_2O_3-Gd_2O_3$ rods were formed and sintered.

3.5 $Al_2O_3-Gd_2O_3$ Reaction Studies

For studies of the reaction between $Al_2O_3-Gd_2O_3$, rods of Al_2O_3 containing Gd_2O_3 particles were formed and sintered.

3.6 Fabrication of $Gd_{23}O_3$ Wafers

Anticipating that thin wafers might be the desired shape of the poison lumps, thin sheets of $Gd_{23}O_3$ were made, punched to form wafers, and sintered.

4.0 DESCRIPTION OF WORK, PHYSICS, AND FABRICATION RESULTS

4.1 Nuclear Cross Section Data

The material properties of gadolinium metal and gadolinia to be used in this study are listed in Table 4.1 below.

TABLE 4.1

MATERIAL PROPERTIES OF GADOLINIUM AND GADOLINIA

<u>Property</u>	<u>Gd</u>	<u>Gd₂O₃</u>
Atomic Weight	156.9	361.8
Density (g/cm ³)	7.895	7.407

Table 4.2 lists cross sections for the stable isotopes of gadolinium as given in Reference 1, and the isotopic abundancies of gadolinium.

TABLE 4.2

GADOLINIUM ISOTOPIIC DATA

<u>Isotope</u>	<u>Abundance (%)</u>	<u>$\sigma_a(2200\text{m/s})$ (barns)</u>
Natural	100	46,000
152	0.20	<125
154	2.15	
155	14.73	56,200 \pm 1000
156	20.47	
157	15.68	242,000 \pm 4000
158	24.87	3.9 \pm 0.4
160	21.90	0.8 \pm 0.3

The data in Tables 4.1 and 4.2 are identical to those used in an earlier study (Ref. 2) for which excellent agreement was obtained between experiment and calculations.

Isotopes 154 and 156 do not activate, and their cross sections have not been measured. Gd-156 is quite significant, as it is present in natural gadolinium, and is produced by neutron capture in Gd-155 for a total concentration of up to 35 per cent in a depleted sample. The work in Reference 2 based on danger coefficient measurements of irradiated samples indicates a Gd-156 thermal cross section of 300 ± 300 barns. Reference 3 lists a Gd-156 upper limit cross section value, as measured by mass spectrographic methods in a thermal reactor, of 14 barns. Thus, until the irradiation experiments proposed in this program are completed, the absorption cross section of Gd-156 will be assumed to be zero.

Measurements by Moller, et al at Brookhaven (Ref. 4) for three gadolinium samples of different isotopic abundances over a range of 0.018 to 1.0 ev yielded the resonance parameters given in Table 4.3.

TABLE 4.3

THERMAL RESONANCE PARAMETERS FOR GADOLINIUM

<u>Isotope</u>	<u>E_0(ev)</u>	<u>Γ(ev)</u>	<u>Γ_γ(ev)</u>	<u>$2g\Gamma_n$(mv)</u>	<u>$2g\Gamma_n^0$(md)</u>
Gd-155	0.0268	0.108	0.108	0.130	0.800
Gd-157	0.0314	0.107	0.106	0.590	3.350

Cross sections for Gd-155 and Gd-157 plotted on Figure 1 are based on the Breit-Wigner single level formula with the resonance parameters of Table 4.3. These curves with the isotopic abundances of Table 4.2 were

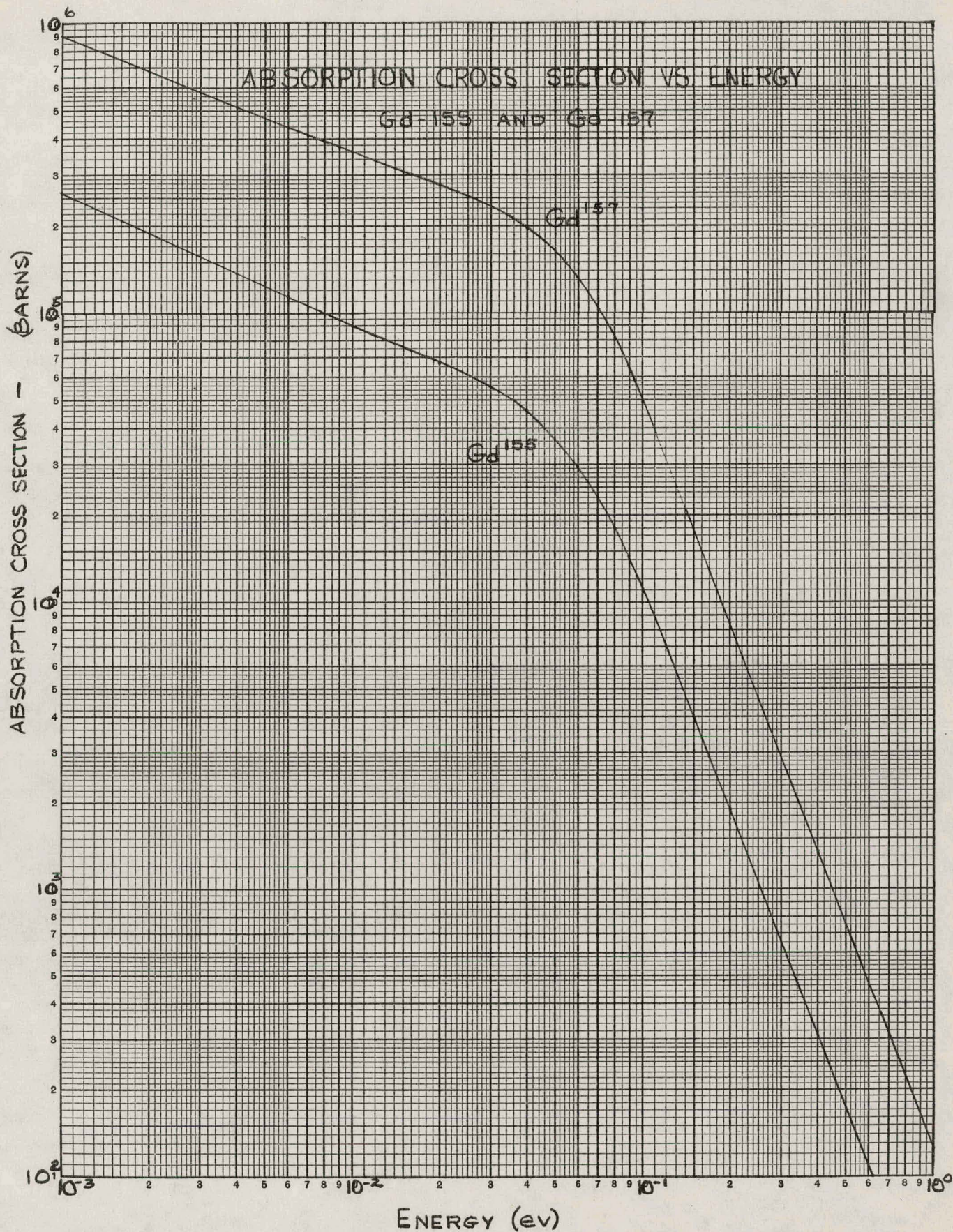


Figure 1 - Absorption Cross Section For Gd-155 and Gd-157

used to compute the natural gadolinium absorption cross section versus energy. These results are compared with the BNL (Ref. 1) curve for natural gadolinium on Figure 2. Comparison of Figures 1 and 2 with Table 4.2 shows that the calculated cross sections are slightly high in the 0.025 ev region.

The isotopic absorption cross sections were averaged over a thermal neutron flux distribution assuming the neutron density distribution to be Maxwellian

$$\phi(E) = AEe^{-E/kT}$$

These results for temperatures from 70 F to 600 F are summarized on Figure 3.

4.2 Poison Demand Curves

To provide a basis for selection of a poison lump shape, poison demand curves were computed as a function of MWD/T for a large boiling water reactor. The poison demand is defined as the poison required to adjust the reactor to criticality in the equilibrium full power operating condition, with all control rods fully withdrawn.

Two group lattice constants and hence the multiplying properties for a large range of boiling water reactor lattices were available from fuel cycle economic studies performed at Allis-Chalmers. To date eight reactor lattices described in Table 4.4 have been analyzed.

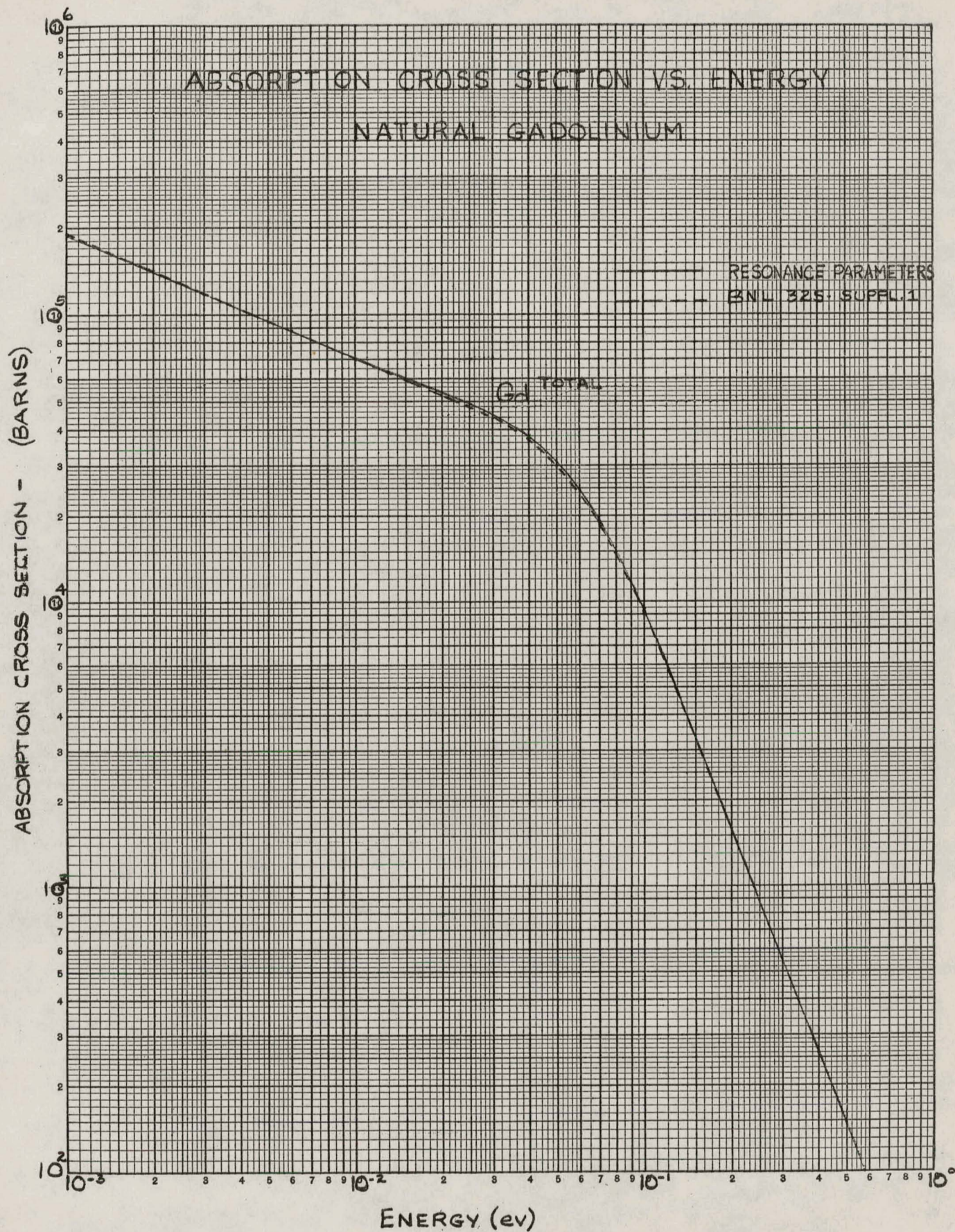


Figure 2 - Absorption Cross Section For Gd Vs. Energy

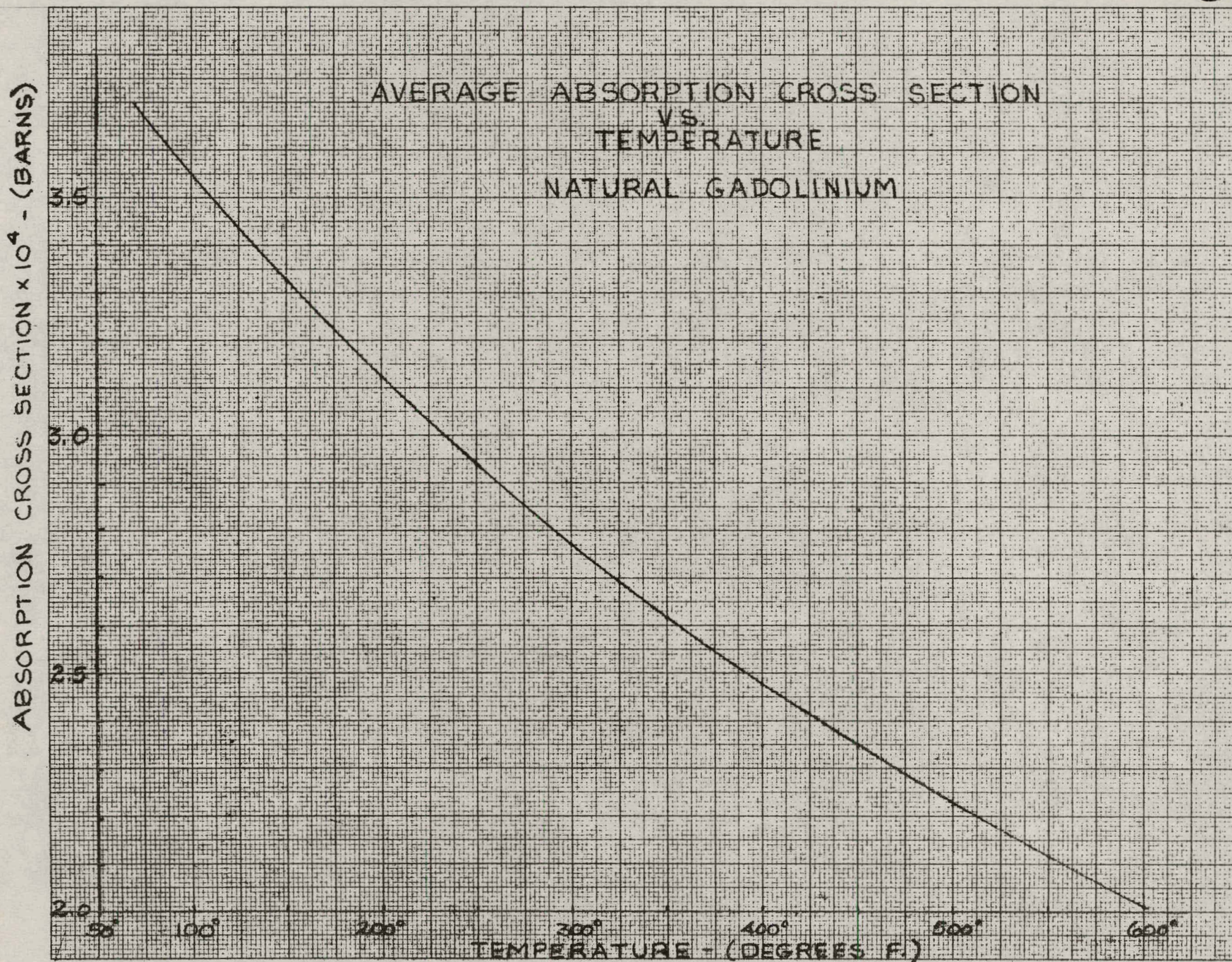


Figure 3 - Maxwellian Averaged Absorption Cross Section for Gd Vs. Temperature

TABLE 4.4

DESCRIPTION OF REACTOR LATTICES FOR
WHICH POISON DEMAND WAS COMPUTED

<u>Parameter</u>	<u>Value</u>
Pressure (psi)	1000
Saturation temperature ($^{\circ}$ F)	545
H ₂ O/UO ₂ volume ratio	2.6
Average void volume fraction	0.30
Fuel rod diameter	0.500
Stainless steel clad	
UO ₂ diameter (inches)	0.459
Clad thickness (inches)	0.019
Enrichment (W/O U-235)	2.3, 2.8, 3.3, and 3.8
Zirconium clad	
UO ₂ diameter (inches)	0.447
Clad thickness (inches)	0.025
Enrichment (W/O U-235)	1.8, 2.3, 2.8, and 3.3

The Allis-Chalmers analytical model for depletion of fuel lattices includes the following:

1. fast group constants for the energy range 0.625 ev to 10 Mev based on the MUFT program,
2. U-238 resonance escape probability with doppler broadening normalized to experimental results,
3. thermal group constants below 0.625 ev based on the SOFOCATE program,

4. thermal group UO_2 , clad, and H_2O flux weighted disadvantage factors computed using the P-3 approximation,
5. long term fission product absorption cross sections in both fast and thermal groups using the data in Reference 5.

For the poison demand, a thermal poison was added uniformly to the fuel lattice, and the thermal component of the two-group infinite multiplication factor adjusted to yield a $k^\infty = 1.03$. The choice of 1.03 allows 0.02 $\Delta k/k$ for leakage (geometric buckling of approximately 0.00025 cm^{-2}) and 0.01 $\Delta k/k$ for non-uniform depletion effects (the depletion calculations were performed using a two-group zero dimensional model). All parasitic absorption due to control rod channels, structure, etc. was included explicitly in the calculations. The poison demand curves for the eight lattices described in Table 4.4 are shown on Figure 4. As the poison demand approaches zero, the reactor becomes subcritical, $k^\infty < 1.03$. Note that over the majority of reactor life, the poison requirements decrease linearly with life. This is especially true for the higher enrichments where the gain in reactivity due to conversion is not apparent.

Fuel depletion is in terms of MWD per metric ton of uranium. The data on Figure 4 assumes complete reactor refueling. If the reactor would be refueled one-third at a time, a more likely situation, the scale on Figure 4 should be divided by 0.67. Thus, 15,000 MWD/T on Figure 4 represents fuel depletion to 22,500 MWD/T with a one-third core refueling schedule.

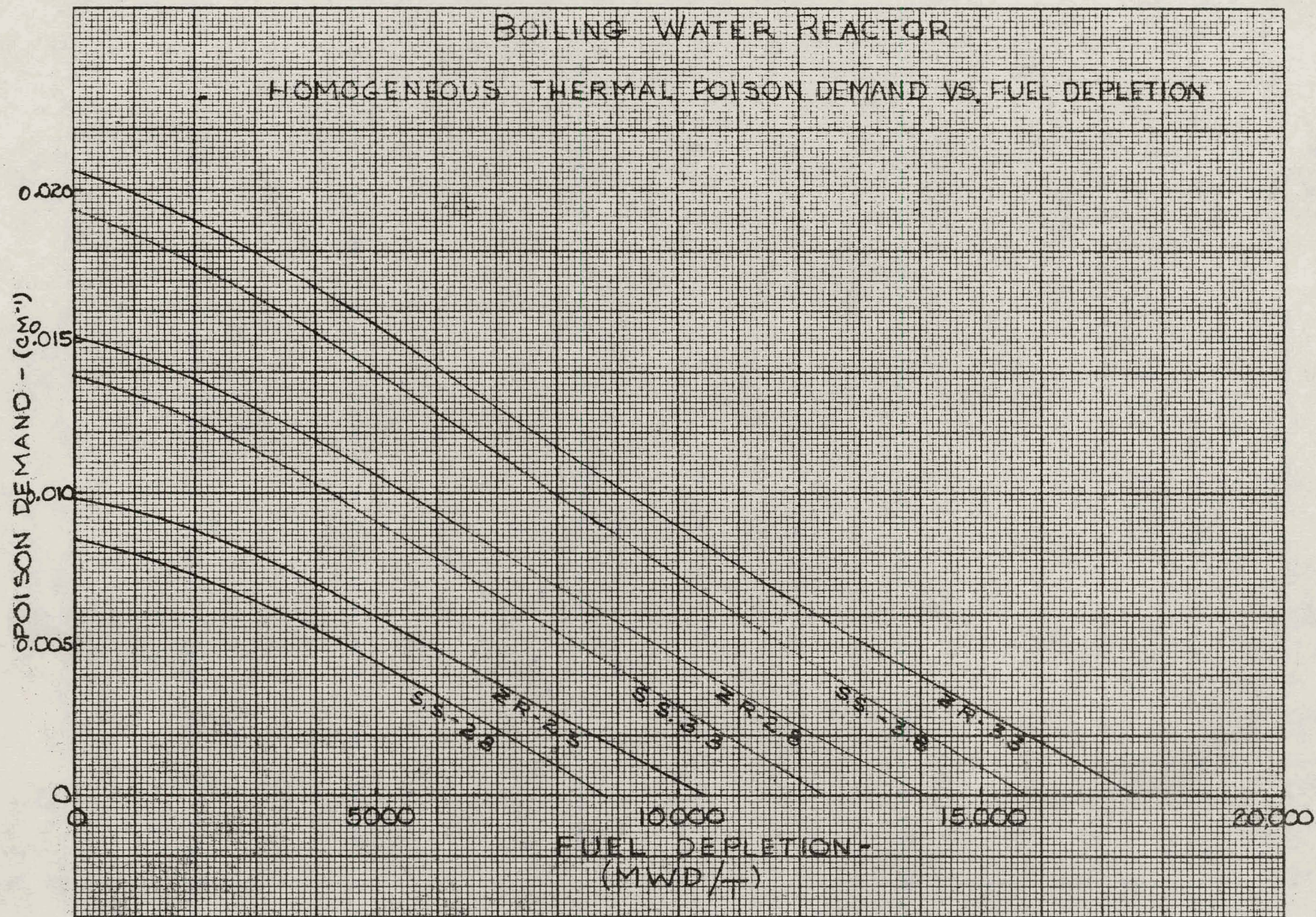


Figure 4 - Poison Demand Curves for Boiling Water Reactor with $H_2O/UO_2 = 2.5$

4.3 Analytical Model for Depletion of Poison Cylinders

The poison demand curves on Figure 4 suggest that the poison lumps be shaped into cylinders. In a preliminary calculation for a poison cylinder, it was assumed that all absorptions occur at the surface.

Here the poison effectiveness is proportional to the radius, and thus varies linearly with irradiation matching the poison demand curves.

To confirm the selection of cylindrical poison lumps, more precise calculations have been initiated. These calculations involve the function

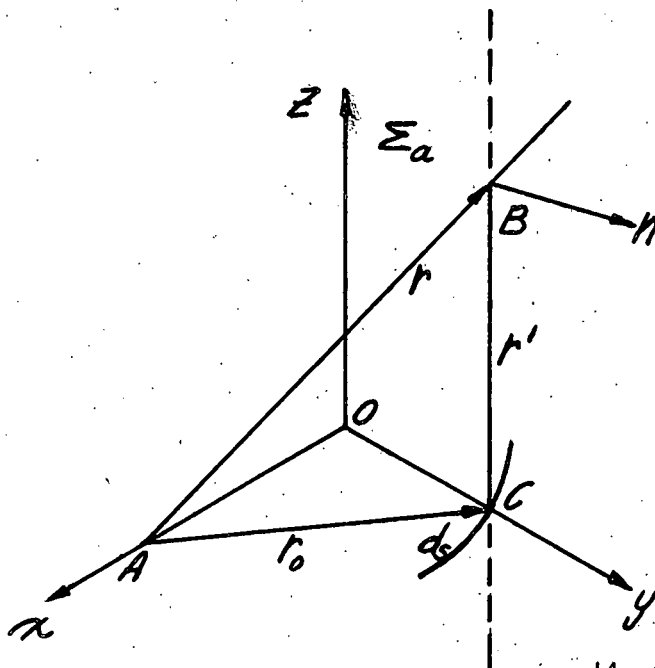
$$F(X) = \int_0^{\infty} X e^{-ux} \frac{\sqrt{u^2 - 1}}{u} du.$$

A literature search has not related this function to existing tables, so the integral will be evaluated numerically.

This function arises from consideration of the probability of neutron escape (Ref. 6) from a cylindrical lump as follows:

For a unit isotropic point source at A in a purely absorbing medium, the probability (P) for a neutron escaping through a surface on B is:

$$dP(r)/ds = 1/4\pi e^{-\Sigma_a r} / r^2 \vec{r} \cdot \vec{n} / r,$$



where:

ds = surface element

\vec{n} = outer normal at ds on B .

If the surface is a cylinder along axis z , n remains constant along

the line CB and $\vec{r} = \vec{r}_0 + \vec{r}'$

$$\vec{r} \cdot \vec{n} = \vec{r}_0 \cdot \vec{n}$$

$$\vec{r} \cdot \vec{n} / |\vec{r}| = \vec{r}_0 \cdot \vec{n} / |\vec{r}|$$

$$ds = \vec{ds} \cdot \vec{dz} - ds \text{ element of length in } xy \text{ plane}$$

Since:

$$dz = d \cdot \sqrt{r^2 - r_0^2}$$

$$dP/ds = \vec{r}_0 \cdot \vec{n} / 4\pi \int e^{-\Sigma_a r} / r^3 d(\sqrt{r^2 - r_0^2}) = \vec{r}_0 \cdot \vec{n} / 4\pi \int e^{-\Sigma_a r} d(\sqrt{r^2 - r_0^2} / r_0^2 r)$$

$$\text{as } 1/r^3 d(\sqrt{r^2 - r_0^2}) = d(\sqrt{r^2 - r_0^2} / r_0^2 r)$$

For an infinite cylinder and for Σ_a independent of z

$$dP/ds = 2 \cdot \vec{r}_0 \cdot \vec{n} / 4\pi \Sigma_a / r_0^2 \int_{r_0}^{\infty} e^{-\Sigma_a r} \sqrt{r^2 - r_0^2} / r dr$$

Let:

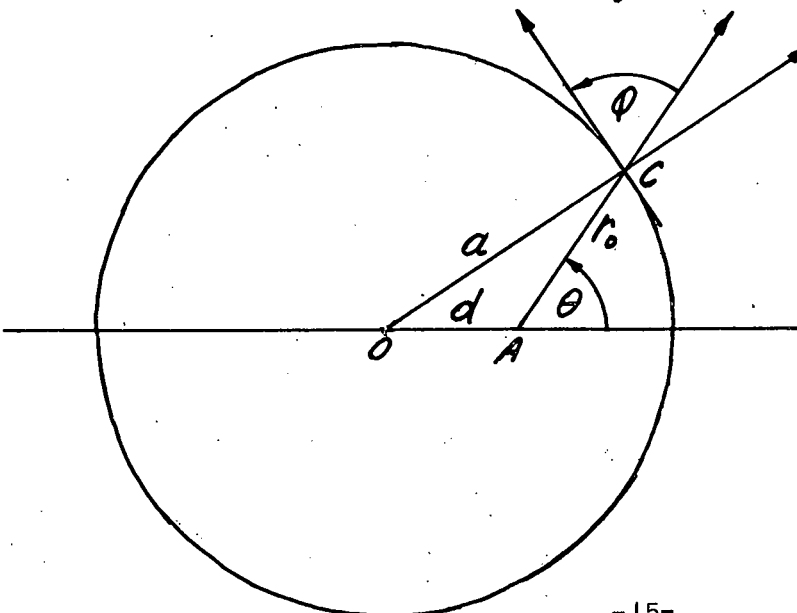
$$x = \Sigma_a r_0$$

and

$$u = r/r_0$$

Then:

$$dP/ds = \vec{r}_0 \cdot \vec{n} / 2\pi \Sigma_a / r_0 \int_1^{\infty} e^{-xu} \sqrt{u^2 - 1} / u du.$$



Next:

take polar coordinate (r, θ) for point C. $\vec{r}_o \cdot \vec{n} / r_o$ is the cosine of the angle between the line AC and the normal to the curve, also equal to the sine of the angle of line AC, and the tangent to the curve

$$\vec{r}_o \cdot \vec{n} / r_o = \sin \varphi$$

we and

$$\sin \varphi = r_o d\theta / ds$$

hence the integral dP/ds becomes

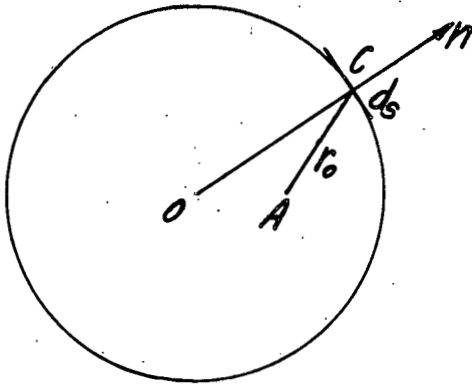
$$dP = \Sigma_a / 2\pi \cdot r_o d\theta \int_1^\infty e^{-xu} \sqrt{u^2 - 1} / u \cdot du$$

$$P = 1/2\pi \int_0^{2\pi} \Sigma_a r_o d\theta \int_1^\infty e^{-xu} \sqrt{u^2 - 1} / u \cdot du$$

$$\Sigma_a r_o = x$$

$$P(x) = 1/2\pi \int_0^{2\pi} d\theta \int_1^\infty x e^{-xu} \sqrt{u^2 - 1} / u \cdot du$$

To obtain the neutron density at A consider the number (ρ) of neutrons escaping from the cylinder is $\rho = \int d\rho / ds \cdot ds$



If the cylinder is immersed in an infinite bath of isotropic neutrons in a vacuum, the number of neutrons of speed v entering the body in a

direction \vec{r} at B is $\rho_{\infty} v/4\pi$ in a purely absorbing medium this number is reduced at A by the factor $e^{-\Sigma_a r}$ and the number of neutrons in the solid angle $d\Omega$ from a surface element ds at B is

$$d\rho v = e^{-\Sigma_a r} \rho_{\infty} v/4\pi d\Omega = \rho_{\infty} v/4\pi e^{-\Sigma_a r/r^2} \frac{\vec{r} \cdot \vec{n}}{|\vec{r}|} ds.$$

$1/\rho_{\infty} v \cdot d\rho v/ds$ is the same as $dP(r)/ds$

thus integrating over ds yields

$$P(r) = \rho(r)/\rho_{\infty}$$

and a relationship has been established between the neutron density at r and the probability of a neutron escaping from the cylindrical lump.

Thus, the neutron absorption rate for each speed (v) may be computed as a function of the cylinder radius. This rate is required for detailed depletion studies at each speed. The one velocity depletion rates will be integrated over the incident neutron spectrum to provide total depletion.

4.4 Reaction Study

A search of the literature pertaining to the reactions of Gd_2O_3 with Al_2O_3 revealed that very little work has been done on this subject. The Russians, Tresvyatskii et al (Ref. 7) have constructed a phase diagram. A copy of this diagram was obtained and studied. It indicates that Gd_2O_3 and Al_2O_3 form a eutectic at 25 mole/o Al_2O_3 and at 75 mole/o Al_2O_3 with eutectic temperatures of 1720 ± 20 C and 1930 ± 20 C, respectively.

Only the 25 mole/o Al_2O_3 eutectic mixtures would be of interest in this study, because its melting point is near the sintering temperature of Al_2O_3 . Lumps of Gd_2O_3 dispersed in Al_2O_3 could be completely destroyed

by an aggressive eutectic reaction. Efforts are being made to lower the sintering temperature of Al_2O_3 , and thereby avoid this occurrence, and to verify the Russian experiment.

Samples which have been fabricated for the reaction study are as follows:

1. samples containing 100% Al_2O_3 ,
2. samples containing 100% Gd_2O_3 ,
3. samples containing 100% Gd_2O_3 particles dispersed in a 100% Al_2O_3 matrix,
4. a homogeneous mixture of 10 w/o Gd_2O_3 powder and 90 w/o Al_2O_3 powder.

These mixes were blended with appropriate binders and lubricants and extruded from a 1/4 inch diameter die. The green rods were dried at 100 C and sliced into pellets 1/2 in. long.

Five rods of each of these sample batches were fired in air at various temperatures and soaking times. Firing cycles completed were at temperatures of 2400 F, 2600 F and 2700 F with soaking periods of two hours in each case. Two other firings were made on the same sample distribution to 2700 F with one soaking time of four hours and a second soaking time of six hours.

The results indicated that the 100 per cent Al_2O_3 was not well sintered, but that it did have enough strength to hold wafers in position in a matrix. The Gd_2O_3 was well sintered and showed much greater shrinkage than the Al_2O_3 . The samples containing Gd_2O_3 particles in an Al_2O_3 matrix fired to 2700 F and soaked for six hours were sectioned, polished and examined under

a microscope. The great difference in shrinkage between the two materials left a void which completely surround the Gd_2O_3 particles. A very thin layer of reaction interface was observed in the samples between the Gd_2O_3 and the Al_2O_3 . There was no evidence of a eutectic reaction at this temperature.

4.5 Fabrication Development

Much of the work done to date to produce samples for the reaction study involved fabrication development. The extrusion of 100 per cent Al_2O_3 and 100 per cent Gd_2O_3 established the procedures for producing rods of these two compositions. The extrusion of the Al_2O_3 rods containing Gd_2O_3 particles established the procedure for producing rods of this composition.

Other compositions extruded were homogeneous mixtures of 10 w/o Gd_2O_3 powder and 90 w/o Al_2O_3 , and compositions of minus 325 mesh Al_2O_3 and "Baymal." Baymal is a colloidal Al_2O_3 which should aid in lowering the sintering temperatures of the minus 325 mesh Al_2O_3 .

All of these compositions were fired on the same schedules as the reaction study pellets. The schedules and the physical properties of the samples are summarized in Table 4.4.

Results indicate that 2700 F for six hours is not sufficient for sintering Al_2O_3 to a high density. The Baymal aided in sintering but not to the extent to which it was hoped. It was, however, a very good aid in the actual extrusion process, and will continue to be used in that respect.

TABLE 4.4

PHYSICAL PROPERTIES OF SAMPLES MADE AND SINTERED FOR REACTION STUDY

No.	Sample Composition			Green Density: % Theoretical	Sintered Densities - % of Theoretical				Remarks
	w/o Al ₂ O ₃	w/o Gd ₂ O ₃	% Baymal		2400 F 2 hr Soak	2600 F 2 hr Soak	2700 F 4 hr Soak	2700 F 6 hr Soak	
1	100	-----	-----	53.86	----	-----	-----	60.36	Densities were not measured on the first three samples because of their chalky appearance and obvious low density.
2	75	-----	25	50.84	-----	-----	-----	55.86	Same as above
3	87.5	-----	12.5	54.90	-----	-----	-----	61.26	Same as above
4	90	-----	10	54.51	-----	-----	-----	60.97	Same as above
5	95	-----	5	55.76	56.25	56.52	59.85	60.80	Sample appears to have greater strength than the others along with a very smooth surface.
8	----	100	-----	40.22	52.61	55.06	63.50	66.49	Sample is well sintered after 6 hrs. at 2700 F. Metallographic exam. showed very fine grained porosity homogeneously dispersed throughout the pellets.
9	80	10	10	45.88	44.18	46.41	49.25	49.86	Sample did not sinter to a hard pellet. The surface is chalky and metallographic exam. showed large voids and coarse grained porosity.

TABLE 4.4 (Continued)

No.	Sample Composition		% Baymal	Green Density: Theoretical	Sintered Densities - % of Theoretical				Remarks
	w/o Al ₂ O ₃	w/o Gd ₂ O ₃			2400 F 2 hr Soak	2600 F 2 hr Soak	2700 F 4 hr Soak	2700 F 6 hr Soak	
10	80	Lumps 10 -8+16 mesh	10	-----	-----	-----	-----	-----	Density data on these samples would be meaningless. Metallographic exam. reveals a large void around each lump of Gd ₂ O ₃ and a very narrow reaction interface.
11	90	10	-----	-----	-----	-----	-----	-----	The softness of this sample indicated that practically no sintering had occurred, so no data or other exam. was made.
12	90	Lumps 10	-----	-----	-----	-----	-----	-----	Sample No. 10 had a better physical appearance than this sample, so no data or other exam. was made.

4.6 Fabrication of Gd_2O_3 Wafers

Four methods were examined in an effort to produce thin wafers of 100 per cent Gd_2O_3 as follows:

1. Dry Pressing:

Fifty grams of Al_2O_3 were mixed with two g of carbowax and 10 g of distilled water. The mixture was blended until enough water had evaporated to cause the material to form small balls. This was considered to be the right consistency for pressing. The batch of material was divided and weighed out into one g samples. The samples were loaded into a 1/4 in. diam. die and pressed with 60 tons per square inch pressure. The pieces produced were very fragile, and the process so slow that this method was abandoned.

2. Extrusion and Slicing:

This method involved the extrusion of Gd_2O_3 into rods of the required diameter and sintering them. After sintering the rods are to be sliced with a diamond or abrasive wheel to the desired thickness. The extrusion part of this process was proved in the reaction study. Attempts to slice the rod will be made in the future.

3. Porous Carrier Technique:

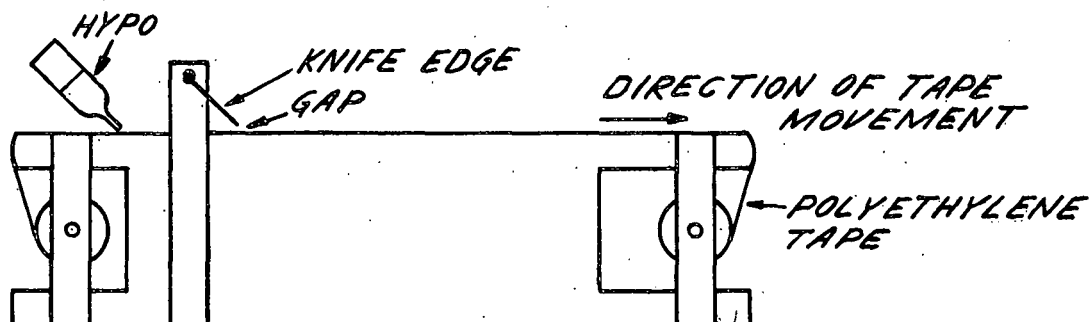
A thick slurry of Gd_2O_3 in water was made. Thin slabs of dry plaster of Paris were dipped into the slurry and held there for different times. The thickness of the coating obtained on

the plaster of Paris slabs was time dependent.

Castings of plaster of Paris are very porous and have a great affinity for water. When they are dipped into a water suspension, the water is absorbed and a layer of solids is left on the surface of the plaster. Due to the extremely small particle size of the Gd_2O_3 , 1.35 μ ; the coatings obtained were tightly adhered to the plaster of Paris slabs and could not be removed intact. As a consequence, this method was abandoned.

4. Non-porous Carrier Technique:

A thick slurry of Gd_2O_3 , Methocel, and distilled water was made and mixed in a high speed impeller type blender until a homogeneous mixture was obtained. The container of slurry was then placed in a vacuum chamber, and 29 inches of Hg. vacuum was drawn on the chamber. After all air bubbles were drawn out of the slurry, the chamber was opened and the slurry container removed. The slurry was poured into a 25 cc. hypodermic syringe and was then extruded onto a polyethylene tape. This apparatus is shown on the following sketch.



The slurry was extruded on the tape, and passed under the knife edge as the roller on the right turned. The knife edge scraped off the excess slurry. The remainder of the slurry formed a film the thickness of the gap. The tape was cut and allowed to dry. The Gd_2O_3 film was removed from the tape, cut into wafers and fired. With this method wafers 0.002 in. thick with a maximum deviation of ± 0.0008 in. were produced. This method appears to be successful.

5.0 PLANS FOR FUTURE WORK

5.1 Poison Demand Curves and Control Requirements

Poison demand curves will be computed for boiling water reactor lattices with H_2O/UO_2 ratios of 2.0 and 3.0, operating pressures of 600 and 2000 psi, void fractions from 0.20 and 0.40, and depletion histories from 10,000 to 25,000 MWD/T. The initial homogeneous poison from the poison demand curves will be converted to poison lumps with the same effective absorption cross section. The behavior of the poison lumps will be calculated as a function of moderator temperature. This will enable an estimate of the fixed absorber poison (control rods) required for core shutdown and regulation from the cold clean to hot operating equilibrium poison conditions. See Figure 5.

5.2 Depletion of Poison Lumps

The development of the calculational model for detailed depletion studies of cylinders will continue. See Figure 5.

5.3 Poison Lumps for Danger Coefficients

The poison samples will be specified for the initial danger coefficient measurements, and fabrication of these samples will begin. See Figure 5.

5.4 Reaction Studies

The $Al_2O_3-Gd_2O_3$ reaction studies will be extended to 3100 F for both Gd_2O_3 particles, and cylinders, and/or wafers in Al_2O_3 to establish the eutectic temperature, and to increase the sintered strength of the Al_2O_3 matrix. See Figure 5.

5.5 Fabrication Techniques

Fabrication techniques for small diameter $Gd_{23}O_3$ cylinders will be developed. More work will be done on the wafer technique to improve the sintered density and to lower the variation in thickness. See Figure 5.

5.6 Danger Coefficient Samples

Fabrication of the samples required for the initial danger coefficient measurements will begin. See Figure 5.

Dec. 1962 Jan. 1963 Feb. Mar. Apr. May June July Aug. Sept. Oct. Nov. Dec. Jan. 1964 Feb. Mar. April May June

PHYSICS

Nuclear Requirements

Gd Cross Section

Poison Demand Curves

Control Requirements

Effective Cross Section

Poison Shapes for Danger Coefficient Measurements

Initial Danger Coefficient Measurements

Analysis of Initial Danger Coefficient Measurements

Irradiation Experiments

Shapes for Irradiation Experiments

Irradiation of Homogeneous Samples

Analysis of Homogeneous Irradiation Data-Final Danger Coefficients

Irradiation of Shaped Samples

Analysis of Shaped Sample Irradiation Final Danger Coefficients

FABRICATION

Reaction Study

Al_2O_3, Gd_2O_3
 $Al_2O_3 - Gd_2O_3$

Rod Fabrication

Evaluation of Results

Fabrication of Gd_2O_3

Form Wafers

Form Cylinders

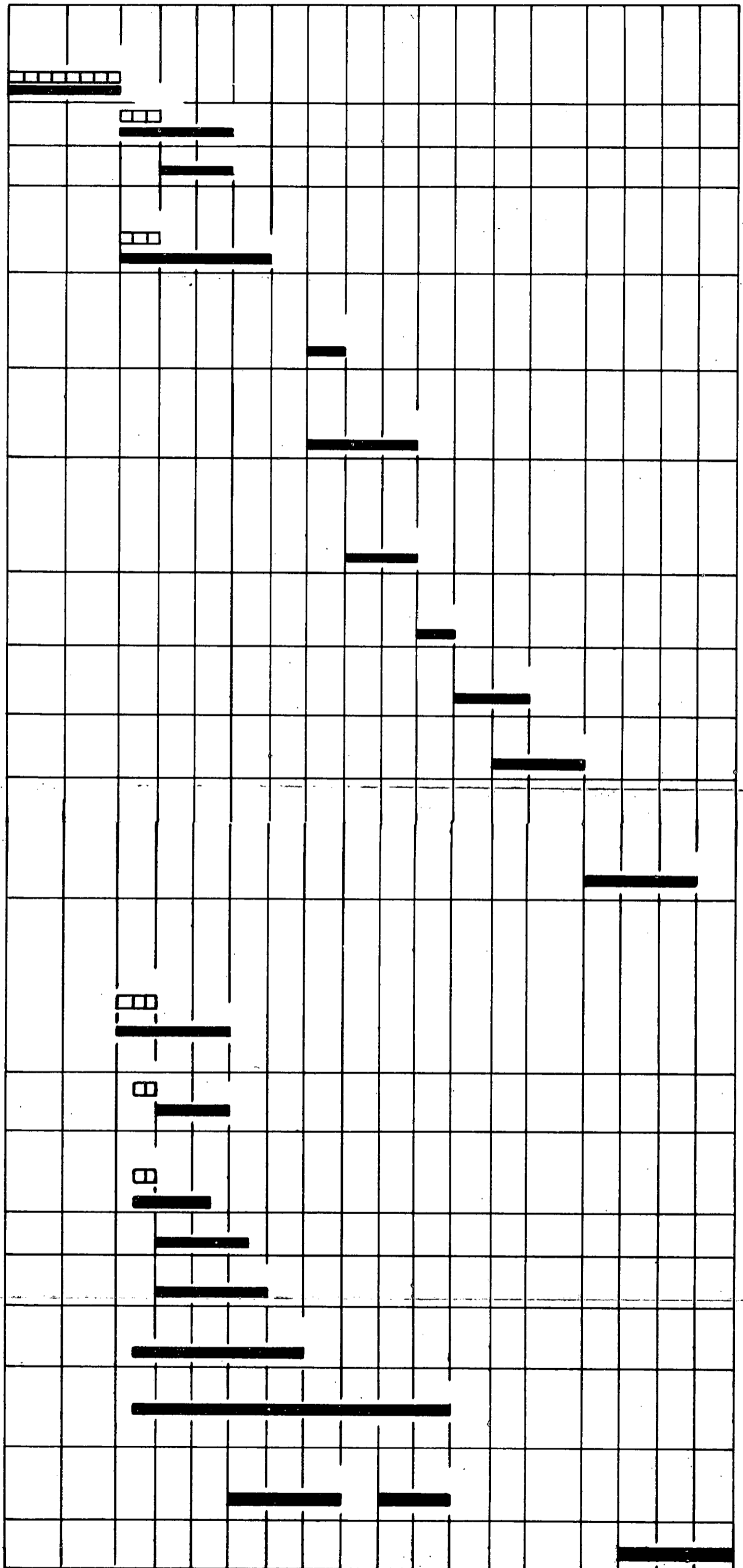
Sinter Wafers and Cylinders

Evaluation of Results

Fabrication of Al_2O_3 Rods Containing Dispersed Gd_2O_3 Lumps

Fabrication of Samples for Physics Tests

FINAL REPORT





 Performance
 Proposed Schedule

FIGURE 5- SCHEDULE OF PROGRESS CHART

6.0 CONCLUSIONS

The analysis to date indicates that for boiling water reactors with low enriched UO_2 fuel, Gd poison lumps cylindrically shaped closely approximate the poison required to match the reactivity loss due to fuel depletion for reactor operation with minimum control rod motion.

The non-porous carrier technique of fabricating Gd_2O_3 wafers appears successful.

REFERENCES

1. Hughes, D. J., Magurno, B. A., and Brussel, M. K., "Neutron Cross Sections," BNL-325, Second Edition, Supplement No. 1, Jan. 1960.
2. Holl, R. J., "Highly Self-Shielded Burnable Poisons," ACNP-63003, March 6, 1963.
3. Hurst, D. G., Kennedy, J. M., and Walker, W. H., "Cross Sections and Yields of Pseudo-Fission Products," CRPP-760.
4. Moller, H. B., Shore, F. J., and Sailer, V. L., "Low Energy Neutron Resonances in Erbium and Gadolinium," Nuclear Science and Engineering, Vol. 8, p. 183, Sept. 1960.
5. Greenhow, C. R. and Hansen, E. C., "Thermal and Resonance Fission-Product Poisoning for U-235 System," KAPL-2172, Oct. 1961.
6. Case, K. M., DeHoffman, F. and Placzek, G., "Introduction to the Theory of Neutron Diffusion," Vol. 1, June, 1953.
7. Tresvyatski, S. G., Kushakovski, V. K., and Belevantsev, V. S., "The $\text{Al}_2\text{O}_3\text{-Sm}_2\text{O}_3$ and $\text{Al}_2\text{O}_3\text{-Gd}_2\text{O}_3$ Systems," Atomnaya Energ., Vol. 9, p. 219, Sept. 1960.